hydrology

MDPI

Article

Soil Moisture Monitoring in Iran by Implementing Satellite Data into the Root-Zone SMAR Model

Fatemeh Gheybi [1,†], Parivash Paridad [2,†], Farid Faridani [1], Ali Farid [1], Alonso Pizarro [2,*], Mauro Fiorentino [2] and Salvatore Manfreda [2]

[1] Department of Water Science and Engineering, Ferdowsi University of Mashhad, Mashhad 91779489, Iran; f.gheybi@mail.um.ac.ir (F.G.); fa.faridani@mail.um.ac.ir (F.F.); farid-h@um.ac.ir (A.F.)

[2] Department of European and Mediterranean Cultures, University of Basilicata, 75100 Matera, Italy; parivash.paridad@unibas.it (P.P.); mauro.fiorentino@unibas.it (M.F.); salvatore.manfreda@unibas.it (S.M.)

* Correspondence: alonso.pizarro@unibas.it

† These authors contributed equally to this work.

Received: 15 March 2019; Accepted: 24 May 2019; Published: 28 May 2019

Abstract: Monitoring Surface Soil Moisture (SSM) and Root Zone Soil Moisture (RZSM) dynamics at the regional scale is of fundamental importance to many hydrological and ecological studies. This need becomes even more critical in arid and semi-arid regions, where there are a lack of in situ observations. In this regard, satellite-based Soil Moisture (SM) data is promising due to the temporal resolution of acquisitions and the spatial coverage of observations. Satellite-based SM products are only able to estimate moisture from the soil top layer; however, linking SSM with RZSM would provide valuable information on land surface-atmosphere interactions. In the present study, satellite-based SSM data from Soil Moisture and Ocean Salinity (SMOS), Advanced Microwave Scanning Radiometer 2 (AMSR2), and Soil Moisture Active Passive (SMAP) are first compared with the few available SM in situ observations, and are then coupled with the Soil Moisture Analytical Relationship (SMAR) model to estimate RZSM in Iran. The comparison between in situ SM observations and satellite data showed that the SMAP satellite products provide more accurate description of SSM with an average correlation coefficient (R) of 0.55, root-mean-square error (RMSE) of 0.078 m^3 m^{-3} and a Bias of 0.033 m^3 m^{-3}. Thereafter, the SMAP satellite products were coupled with SMAR model, providing a description of the RZSM with performances that are strongly influenced by the misalignment between point and pixel processes measured in the preliminary comparison of SSM data.

Keywords: surface soil moisture; root-zone soil moisture; remote sensing; SMAR

1. Introduction

Soil Moisture (SM) is a connective hydrological variable between the Earth's surface and the atmosphere, being dominant on various climatological processes through its role in Evapotranspiration (ET), runoff and groundwater recharge [1–5]. In turn, detailed information on SM aims at improving climatic predictions and meteorological models, influencing activities such as water resources management, agriculture efficiency, irrigation planning, and prevention of natural hazards [6–10].

The discrete nature of direct observation methods precludes the spatial distribution of SM due to its temporal and spatial variability; moreover, these methods require qualified operators, which makes them costly and time-consuming [11]. In this context, the application of remotely-sensed products has become an alternative for large-scale SM monitoring [12]. While visible methods are based on the soil surface reflectance, thermal infrared methods function on the sensitivity of land surface temperature (LST) to Surface Soil Moisture SSM [4]. Remote sensing methods based on microwave radiation have been applied through active or passive sensors. Remotely-sensed SM products through microwave

emissions are widely investigated in many researches due to their potentials for monitoring SM in all temporal and meteorological conditions and the infiltration ability of microwave emissions in sparse vegetation covers. This method functions based on the high level of difference between the soil and water dielectric constants. Solar illumination and cloud cover do not influence microwave remote sensing technique, and its longer wavelengths are not susceptible to atmospheric scattering. Thus, it was considered as the most effective method in remote sensing of SM [11,13]. In recent years, the surface-reflected Global Navigation Satellite System (GNSS) signals have also been evaluated for SM estimations, which applies a different source of signals from the active/passive microwave sensors to observe the Earth's surface [14]. Moreover, the Advanced Scatterometer (ASCAT), which is an active microwave remote sensing instrument, provides global SM data sets derived from the backscatter measurements [15,16].

SM products obtained from active/passive microwave remotely-sensed data have been applied in wide spectra of contexts [17–26]. However, SM data derived from most of the satellite sources provide the near surface moisture that needs to be converted in Root Zone Soil Moisture (RZSM) estimations [27,28]. Recently, high-resolution observations of RZSM have become available through the NASA Airborne Microwave Observatory of Subcanopy and Subsurface (AirMOSS), which have been compared with the microwave remote sensing observations obtained from NASA Soil Moisture Active-Passive (SMAP) mission [29,30]. A more straightforward type of RZSM modelling approach is the use of an exponential filter to predict RZSM from satellite data [31,32]. In this regard, one of the recent models is the Soil Moisture Analytical Relationship (SMAR), developed by Manfreda et al., 2014 and tested with satellite data [32–35].

Despite the importance of water in arid and semi-arid regions, there are only a few studies regarding the evaluation and monitoring of environmental parameters in Iran [36–40]. In particular, a multiyear SSM dataset was extracted from SMOSL3, ECV-SM ERA-Interim and ERA-Interim/Land SSM products in 2015 over six sub regions of Iran with meteorological data characterized by different climate conditions [41]. Their results showed that all SSM products were in good agreement between each other and with in situ precipitation and temperature measurements.

This paper aims to introduce the current status of soil-moisture monitoring in Iran and further improve the evaluation of satellite-based SM products with the intention of understanding SM spatio-temporal variability in semi-arid regions. For this purpose, three different satellite-based SSM data were compared with observed data obtained from five stations in order to evaluate the reliability of different remote sensing products. Afterwards, satellite products were applied to run the SMAR model in order to define the best strategy to describe RZSM in this poorly monitored area.

2. Materials and Methods

2.1. Study Area

Iran can be divided into eight Ecoregions characterized by different annual rainfalls, with an average of 260 mm (Figure 1) [42,43]. Each ecoregion is characterized by different rainfall regimes with the driest located in the south-eastern part of the country (Zone 1), while the northern area at the margins of the Caspian Sea receives the highest amount of annual rainfall (Zones 6 and 8).

2.2. In Situ Data

The entire country is monitored with few Agro-Meteorological (AM) stations (about 23 AM stations) that measure climatic data and also SM. In particular, SM measurements are taken at different depths using Time-domain reflectometry (TDR) or gravimetric method on a daily to weekly basis. The compact data logger applied was COMBILOG 1020 by Theodor Friedrichs & Co. GmbH from Schenefeld (Germany), which records various measurements such as temperature, wind speed and soil moisture. The spatial distribution of the AM stations is described in Figure 1 [44].

The quality of the data is generally poor with several gaps in time series and biases due to the manual operation of data collection. Therefore, only five of these stations provide reliable time series that can be used for the subsequent analyses. Information regarding each study site is presented in Table 1, which provides geographical location, elevation, soil texture, measurement depths, and mean annual precipitation [45]. Sparse agricultural crops and herbaceous plants cover most of the study sites. The climate condition in all stations is cold and semi-arid except for Oltan station, which is located in a mild and semi-arid region. Kahriz station is located near Lake Urmia; therefore, the lake influences some parameters such as temperature and humidity.

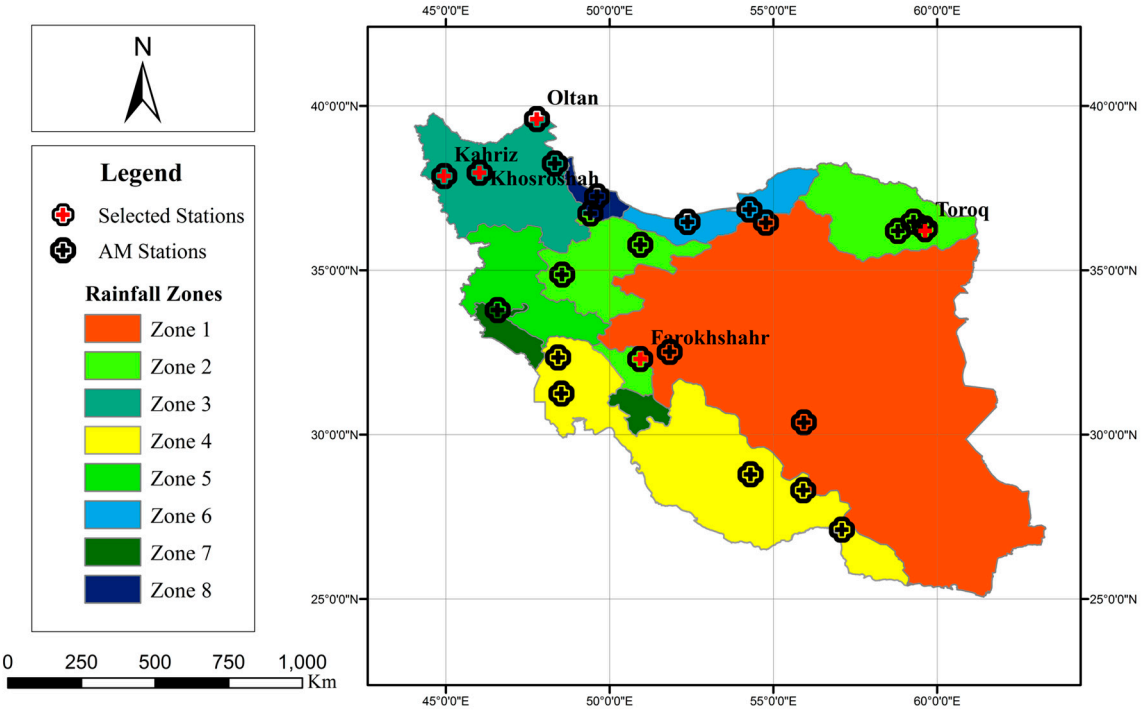

Figure 1. Location of the Agro-Meteorological (AM) stations in eight Ecoregions of Iran (black and red symbols) and the selected stations (red symbols).

Figure 2 shows the time series of SM profile of the five selected stations. The stations are located in two of the eight Ecoregions presented in Figure 1. The Farokhshahr and Toroq stations belong to zone 2, while the Kahriz, Khosroshah, and Oltan stations belong to zone 3. SM dynamics reflects the rainfall pattern of these zones; however, Farokhshahr and Khosroshah display significant differences in the observed dynamics with lower infiltration in the lower soil layers.

Table 1. Characteristics of each monitoring station adopted in the study.

Station Name	Latitude	Longitude	Elevation (m)	Soil Texture	Measurement Depths (cm)	Mean Annual Precipitation (mm/year)
Farokhshahr	32.30	50.93	1636	Loam	5, 10, 30, 50	300
Kahriz	37.88	45.00	1336	Sandy clay	5, 10, 30, 50	313
Khosroshah	37.97	46.04	1338	Sandy loam	5, 10, 20, 30, 50	288
Oltan	39.60	47.76	73	Sandy clay	5, 10, 20, 30, 50	263
Toroq	36.27	59.63	990	Loamy sand	5, 10, 20, 30, 50	233

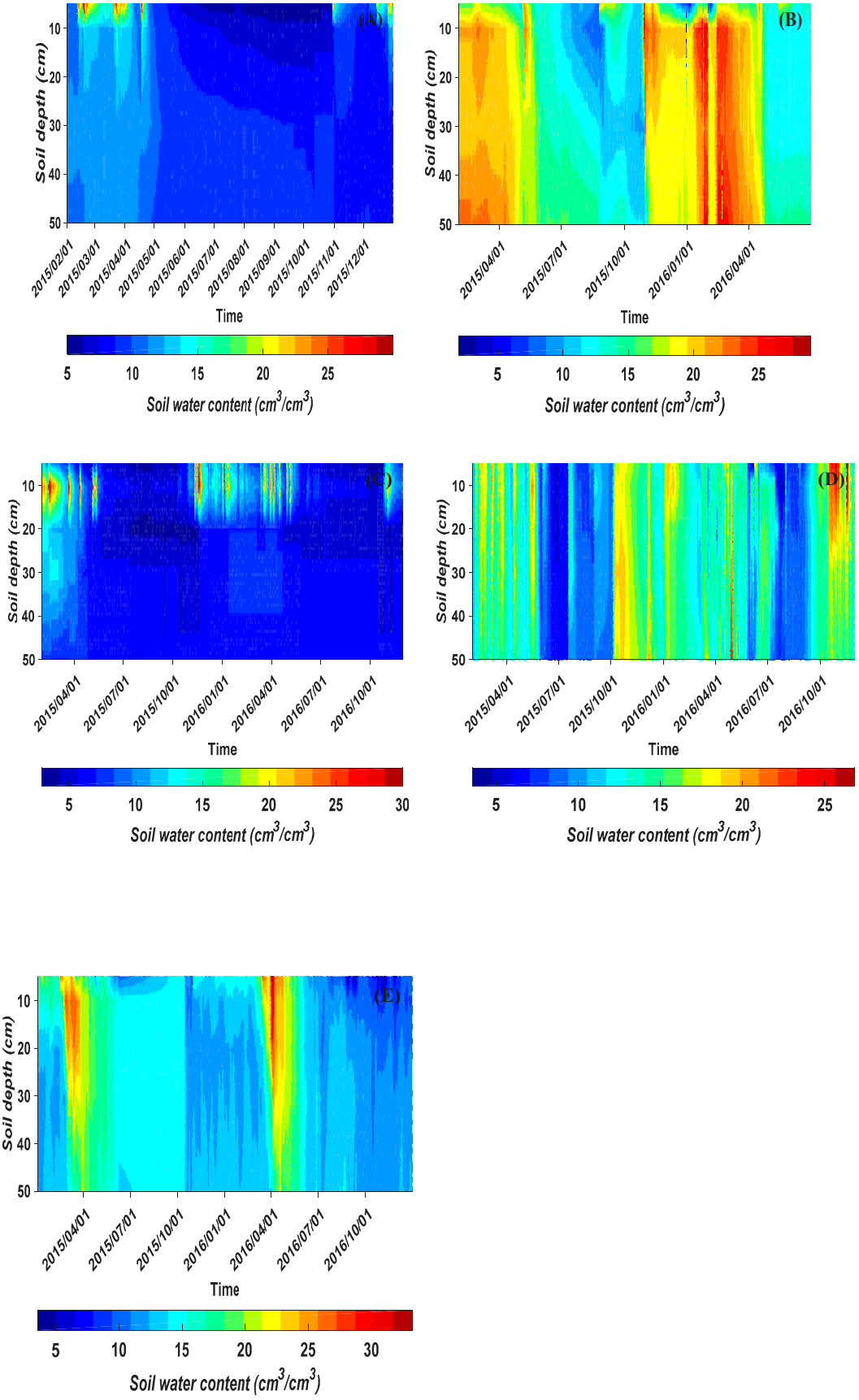

Figure 2. Soil Moisture (SM) dynamics along the soil profile and over the period 2015–2016 for the stations of (**A**) Farokhshahr; (**B**) Kahriz; (**C**) Khosroshah; (**D**) Oltan; (**E**) Toroq.

In situ observations at different depths were applied to describe SM dynamics over the considered study area. SSM was estimated using the measurements taken at surface, while, RZSM was calculated as the weighted average of available SM measurements at different depths.

2.3. Satellite Data

In recent decades, various sensors with microwave technology have been launched to remotely monitor SM. In this research, we applied three SSM products from Soil Moisture and Ocean Salinity (SMOS), Advanced Microwave Scanning Radiometer 2 (AMSR2), and Soil Moisture Active Passive (SMAP) [46–48].

The AMSR2 sensor, developed by the Japanese Aerospace Exploration Agency (JAXA), was launched in 2012 aboard GCOM-W1 [49]. AMSR2 is a passive microwave radiometer that retrieves the SSM both in C and X bands (with 62 km × 35 km, 42 km × 24 km resolution, respectively) every 1 to 2 days from ascending (1.30 P.M. local time) and descending (1.30 A.M. local time) overpasses. AMSR2 SSM products are retrieved from the JAXA (X band only) and Land Parameter Retrieval Model (LPRM) (both C- and X band) algorithms [50]. In this research, SSM products by LPRM from X band (10.7 GHz) with a grid resolution of 0.25 degree were evaluated for the period from 2015 to 2016 [51].

SM estimation using L-band radiometry is a new step in this field since L-band microwave sensors provide maximum sensitivity to SM [52]. ESA's SMOS and NASA's SMAP were launched in 2010 and 2015, respectively, to measure SM at a global scale in L-band [47,48]. SMOS mission observes SM over land and salinity over oceans with the aim to provide global maps every 3 days with a 50 km ground resolution, and volumetric SM every 2 to 3 days with the accuracy of a 0.04 m^3/m^3 [53]. In this study, SMOS L3 daily products (v300) from the Centre Aval de Traitement des Données SMOS (CATDS) with a grid resolution of 25 km including both ascending (6:00 A.M.) and descending (6:00 P.M.) overpasses were used for a time period of 2015–2016 [54].

SMAP, launched by NASA on 31 January 2015, applies a combination of active radar and a passive radiometer in order to measure SM and freeze/thaw at a global scale [48]. SMAP observes Earth's surface from 6:00 A.M. (descending) and 6:00 P.M. (ascending) overpasses and provides global coverage every 1 to 3 days. The SMAP radar stopped transmitting on 7 July 2015 and currently, SMAP only provides SM products from the radiometer. In this research, level 3 SMAP SM products for both ascending/descending overpasses were used during 2015–2016. These products (L3-SM-P) resampled to a global 36 km gridding resolution are available on NASA National Snow and Ice Data Centre Distributed Active Archive Centre (NSIDC DAAC) website [55].

For evaluation of remotely-sensed SM data, SSM values corresponding to each station were extracted using Matlab software. Day and night datasets were integrated in order to fill the time series with all available dates. In case two values were available in the same day (day and night), a simple arithmetic mean was calculated as reference value.

2.4. Soil Moisture Analytical Relationship (SMAR) Model

SMAR model predicts the RZSM based on SSM time series using an analytical relationship developed by Manfreda et al. [33]. The SMAR equation describes the analytical relationship between SSM (s_1) and RZSM (s_2):

$$s_2\left(t_j\right) = s_{w2} + \left(s_2\left(t_{j-1}\right) - s_{w2}\right)e^{-a\left(t_j - t_{j-1}\right)} + (1 - s_{w2})b\ \mathrm{y}\left(t_j\right)\left(t_j - t_{j-1}\right). \quad (1)$$

The function adopts a term $y(t)$ [–] that represents the fraction of soil saturation infiltrating in the lower layer of soil. It assumes the form:

$$y[s_1(t), t] = \begin{cases} (s_1(t) - s_{c1}), & s_1(t) \geq s_{c1} \\ 0, & s_1(t) < s_{c1} \end{cases} \quad (2)$$

where $a = \frac{V_2}{(1-s_{W2})n_2 Zr_2}$ is a normalized daily root zone water loss coefficient, $b = \frac{n_1 Zr_1}{(1-s_{W2})n_2 Zr_2}$ is a normalized coefficient controlling diffusion rate of excess soil moisture, n_1 [–] is soil porosity of the first soil layer, Z_{r1} [L] is depth of the first layer, s_1 (θ_1/n_1) [–] is relative saturation of the first layer, s_{c1} [–] is relative saturation value at field capacity of the first layer of soil, s_2 [–] represents the relative saturation of the second layer, s_{w2} [–] is the relative saturation of the second layer at wilting point, n_2 [–] is soil porosity of second layer, Z_{r2} [L] is the depth of second layer, V_2 [LT^{-1}] is the soil water loss coefficient accounting for both ET and percolation losses, and finally t_j represent time.

SMAR represents a SM analytical relationship between the two state variables introduced with the physically consistent parameters. Model parameters can be estimated exploiting physical information or calibration using RZSM data. It should be noted that SMAR may produce values higher than 1 and in consequence, these are automatically set equal to 1. It is necessary to take into account the potential effect of runoff that is neglected in the mathematical formulation.

2.5. Root Zone Soil Moisture Estimations

Following Faridani et al. [32], SMAR model was applied using three different approaches. SMAR model includes various parameters, which may be estimated considering soil texture information and climate conditions in the region. In the present application, range of parameters was set based on physical characteristics of the sites, but their values were calibrated using both point scale measurements and satellite data. An optimization procedure was carried out to calibrate the model using a genetic algorithm function that adopts the root mean square error (RMSE) as the objective function.

The three schemes have been adopted:

- **Scheme i:** SMAR model is used exploiting as input the time series of in situ SSM data and it is calibrated with the values of in situ observations of RZSM (i.e., point scale application);
- **Scheme ii:** SMAR model is used exploiting as input the time series of satellite SSM data and it is calibrated with the values of in situ observations of RZSM (i.e., pixel scale application);
- **Scheme iii:** SMAR model is used exploiting as input the time series of satellite SSM data, but parameters are assigned using the same values obtained from the point scale/scheme i (i.e., an extension of in situ point parametrization to the pixel scale.)

Model performances were quantified through the correlation coefficient (R), RMSE, and bias [56].

3. Results and Discussion

3.1. Evaluation of Remotely-Sensed Data

SSM level 3 products obtained from three chosen satellites, namely SMAP, SMOS, and AMSR2 over a time period of 2015 to 2016 were compared with SSM measurements in the studied stations in Figure 3. Since most passive satellite sensors cannot observe deeper than a few centimeters [38], the SM measured at the depth of 10 cm was considered as the reference SSM (associated with the first layer of soil in SMAR schematization).

The scatterplots and time series of different SM observations have been depicted in order to provide a preliminary check of data. Table 2 indicates the validation results of all satellite products with observed data in terms of R, RMSE, and Bias statistical indices. We must acknowledge that the comparison is strongly affected by the reference scale of the two measurements (in situ vs. satellite) that may significantly differ because of the internal spatial heterogeneity of soil or land use. Nevertheless, the in situ measurements available were limited in space, and this was the only comparison possible that could provide information about the evolution of soil moisture and an indication on the discriminatory capacity of different sensors.

The direct comparison of the two datasets showed significant variability among the different remotely sensed data. SM products obtained from SMAP were more consistent compared to other sensors and showed closer agreement with in situ observations (with and average R = 0.55 and

RMSE = 0.078 m^3 m^{-3}). AMSR2 and SMOS provided progressively a lower correlation with local measurements with values that move from 0.49 to 0.34. All evaluated sensors showed an overestimation with regards to the observed SSM data in the studied areas.

Table 2. Comparison between remotely sensed and observed SM data expressed in terms of R, root-mean-square error RMSE (m^3 m^{-3}) and Bias (m^3 m^{-3}). In addition, the number of measurements is also provided (N).

	AMSR2				SMOS				SMAP			
Stations	**R**	**RMSE**	**BIAS**	**N**	**R**	**RMSE**	**BIAS**	**N**	**R**	**RMSE**	**BIAS**	**N**
Farokhshahr	0.57	0.143	0.128	306	0.30	0.093	0.030	134	0.40	0.039	−0.010	191
Kahriz	-	-	-	-	0.32	0.115	−0.032	159	0.39	0.135	0.123	195
Khosroshah	0.26	0.100	0.046	524	0.47	0.156	0.088	362	0.67	0.069	0.046	339
Oltan	0.70	0.210	0.178	533	0.29	0.148	0.083	384	0.74	0.075	0.058	243
Toroq	0.45	0.089	0.023	303	0.34	0.084	−0.035	127	0.56	0.070	−0.051	130
Average	0.49	0.135	0.094	417	0.34	0.119	0.027	233	0.55	0.078	0.033	220

Time series in Figure 3 show that AMSR2 tended to overestimate SSM with a positive bias in all stations. This result is also confirmed by previous studies [57,58]. However, in stations with lower moisture values (Toroq and Khosroshah), AMSR2 provided more precise description of local fluctuations of SM.

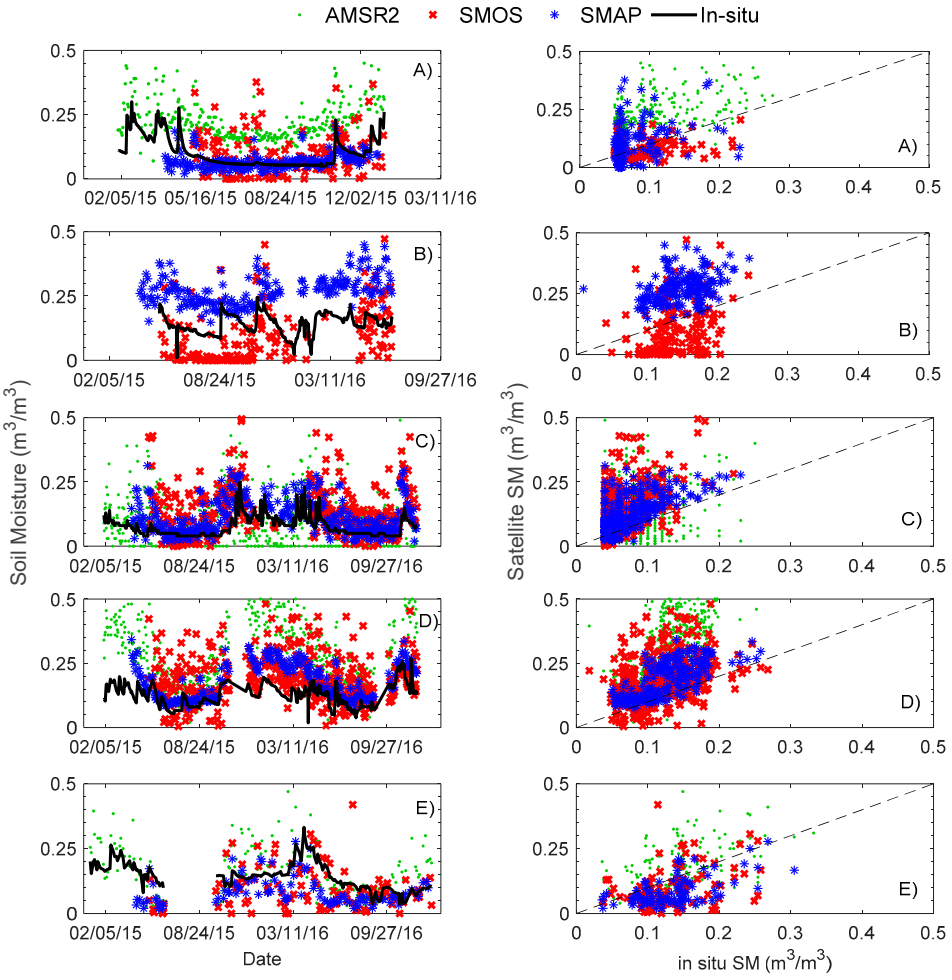

Figure 3. Temporal evolution of SM (left) and Scatterplots (right) of remotely sensed data and measured Surface Soil Moisture (SSM) data in the five stations of (**A**) Farokhshahr; (**B**) Kahriz; (**C**) Khosroshah; (**D**) Oltan; (**E**) Toroq. Dashed lines in Scatterplots represent the ideal line of a perfect agreement.

SMOS measurements showed the higher dispersion respect to local measurements with a correlation coefficient ranging from 0.29 to 0.47. Therefore, SMOS provided the least useful information in terms of SSM with a precision lower than the targeted for the sensor (RMSE < 0.04 m^3 m^{-3}) [55]. Such low performances are also confirmed by the studies performed by Oliva et al., 2012 and Khazaal et al., 2014, who suggested that SMOS faces radiometric interferences in some areas such as the Middle East [59,60].

In conclusion, SSM estimations performed by SMAP satellite provided the best accuracy for the considered dataset. Performances were still not fully satisfying respect to expected precision of the sensor (RMSE < 0.04 m^3 m^{-3}). RMSE values obtained by SMAP assumed an average value of 0.078 m^3m^{-3} and showed an overestimation of +0.033 m^3 m^{-3} (mean bias). In conclusion, SMAP described well the seasonal and temporal SSM fluctuations and showed a lower mean RMSE. As a consequence, SMAP data were chosen to be applied in the next steps as inputs for the SMAR model. SMAP products dominance regarding the other remotely-sensed data and its ability to estimate SSM frequencies has been also mentioned in many other similar investigations [61–63].

3.2. Application of the SMAR Model

As mentioned in Section 2.5, the performance of SMAR model in estimating RZSM was evaluated using three different schemes with the aim to explore the impact of different scales of application on model performances. A summary of the performances in terms of R, RMSE and Bias is given in Table 3 along with the estimated parameters for each of the proposed schemes.

SMAR model was applied at daily scale in all station except for Toroq, where the time-step ($t_j - t_{j-1}$) in Equation (2) was set equal to 3 days and/or 4 days as a function of the available in situ measurements. Time series of RZSM predicted with the three mentioned SMAR schemes and measured in situ data at one point are depicted in Figure 4.

Table 3. Statistical indices and Soil Moisture Analytical Relationship (SMAR) model parameters for the three schemes in all stations.

Station	Schemes	n_1	n_2	s_{c1}	s_{w2}	V_2 (m/day)	R	RMSE (m^3 m^{-3})	Bias (m^3 m^{-3})
Farokhshahr	i	0.497	0.530	0.247	0.170	0.0096	0.9254	0.0119	0.0045
	ii	0.467	0.467	0.476	0.183	0.0057	0.9782	0.0045	−0.0002
	iii	0.497	0.530	0.247	0.170	0.0096	0.544	0.0313	0.0247
Kahriz	i	0.462	0.529	0.388	0.248	0.0198	0.9150	0.0303	0.0004
	ii	0.466	0.530	0.467	0.219	0.0250	0.2813	0.1430	0.0871
	iii	0.462	0.529	0.388	0.248	0.0198	0.2920	0.3209	0.2879
Khosroshah	i	0.500	0.520	0.430	0.122	0.0113	0.8524	0.0184	0.0025
	ii	0.484	0.530	0.477	0.112	0.0056	0.5975	0.0257	0.0118
	iii	0.500	0.520	0.430	0.122	0.0113	0.5057	0.0314	0.0151
Oltan	i	0.452	0.430	0.241	0.215	0.0249	0.8066	0.0459	0.0068
	ii	0.433	0.470	0.436	0.211	0.0250	0.6526	0.1000	0.0487
	iii	0.452	0.430	0.241	0.215	0.0249	0.7677	0.2450	0.1820
Toroq	i	0.490	0.530	0.289	0.237	0.019	0.9463	0.0146	0.0003
	ii	0.444	0.508	0.421	0.241	0.0051	0.9225	0.0174	0.0006
	iii	0.490	0.530	0.289	0.237	0.019	0.7521	0.0291	0.0018

In general, scheme (i) had the best performance in estimating the RZSM in all stations. Scheme (ii) was also quite successful, while scheme (iii) produces unrealistic results. Obviously, the first scheme adopts two time series that are coherent with the structure of the model and its good performances are expected. The second scheme forces the model parametrization to replicate the time series of in situ point scale RZSM, but obviously the critical differences between the two datasets in terms of scale diminishes the quality of the results. Nevertheless, the second scheme produces relatively good results

with set of parameters slightly different respect to the first scheme. Finally, scheme iii demonstrates that the parametrization derived from point scale observations is clearly not compatible with the use of satellite data as input given the strong differences in the reference scale.

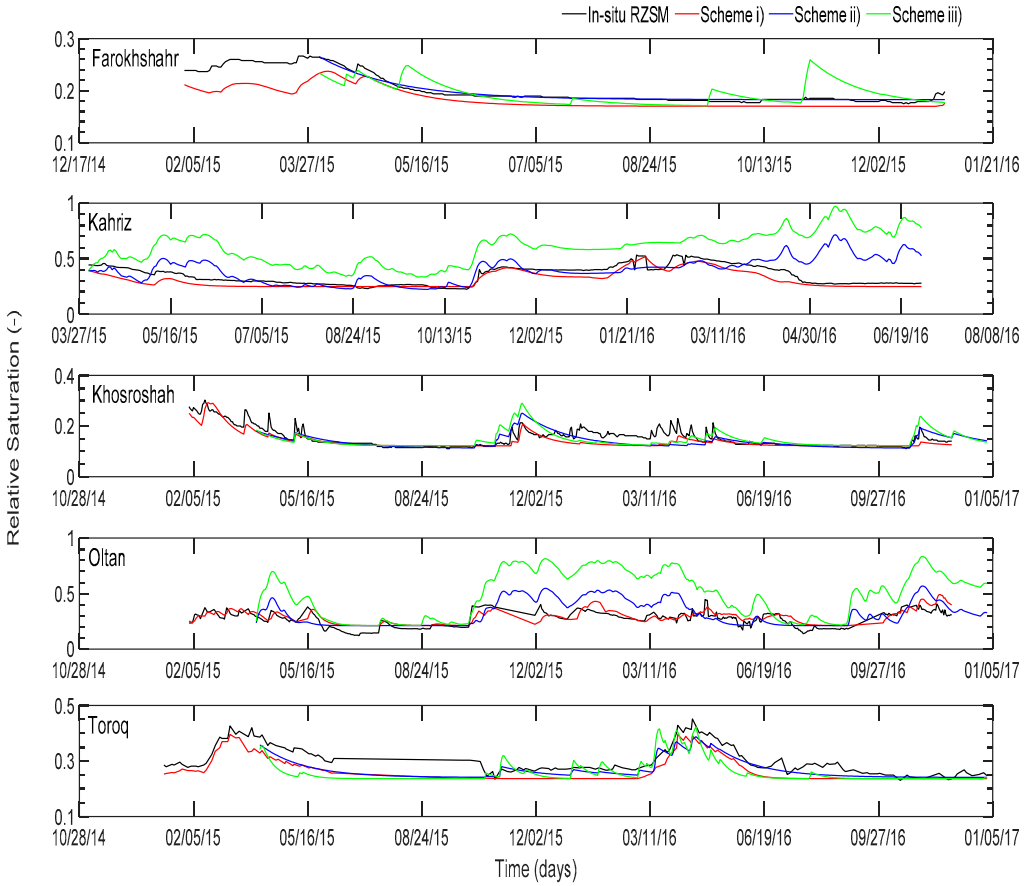

Figure 4. Time series of measured Root Zone Soil Moisture (RZSM) data and SMAR model estimations in the three approaches.

It is interesting to observe that some of the SMAR's parameters, such as n_1, n_2, and s_{w2}, display a small variability moving from scheme (i) to (ii), while V_2 and s_{c1} display a significant sensitivity respect to the input time series of SSM. Therefore, the two parameters V_2 and s_{c1} are more influenced by the change of scale and are also able to force using satellite time series of SSM as input. For instance, the overestimation of the satellite-based SSM data produces as a consequence, higher values of the parameter field capacity of the surface layer (s_{c1}).

More specifically, some differences in model performances were observed between different stations especially for scheme (ii). Such differences may be due to the relative agreement between the time series of SSM. Such differences can be due to the fact that the in situ station is not representative of the dynamics of the satellite pixel. Therefore, the performance of SMAR improves as the correlation between the two increase (compare results in Tables 2 and 3).

4. Conclusions

Iran deals with climate change and a severe shortage of water resources. Therefore, monitoring SSM and RZSM helps to understand important hydrological and ecological processes; leading to mitigate the potential negative impacts of above-mentioned crises. This paper deals with the use of satellite sensors in order to monitor SM in Iran considering the available in situ observations and satellite data (i.e., SMOS, SMAP, and AMSR2).

SM is measured using TDR or gravimetric methods in 23 AM stations at 3–5 depths, but only five of them provide continuous time series. Therefore, analyses presented are strongly limited by the available dataset that is also limited in spatial coverage of in situ observations and also quality of data. These limitations clearly identify an urgent need to increase the number of AM stations and to equip them with proper automatic SM measuring devices (e.g., TDR with data logger) in the region. Nevertheless, the available data were exploited to provide a preliminary evaluation on the satellite products available for SM monitoring in Iran.

Through comparison between SSM of in situ observations and pixel scale SSM, it was possible to rank the reliability of different satellite products. The direct comparison between a point and a pixel value performed herein cannot be considered as a measure of accuracy of satellite products since the spatial variability within the pixel was completely neglected. Therefore, analysis provided only a qualitative analysis that identifies the SMAP products as the most appropriate for Iran.

In consequence, the SMAP data was implemented into the SMAR model to provide a description of RZSM at the in situ-point and at the pixel-scale. Analyses showed that SMAR provided fairly good results especially when applied directly at the point scale using consistent time series. RZSM predictions based on satellite SSM were influenced by the existing correlation with the point scale dynamics, but the temporal pattern is well interpreted.

Due to the lack of SM measuring stations and the poor quality of the available data in regions like Iran, remote sensing techniques represent a viable strategy for SM monitoring in scars-data regions. The proposed study represents a preliminary attempt to address this issue identifying possible strategies and products to further explore in order to provide an alternative methodology for RZSM monitoring in arid and semi-arid areas such as Iran.

Author Contributions: Conceptualization, F.F.; Data curation, F.G.; Formal analysis, F.G. and P.P.; Funding acquisition, S.M.; Investigation, F.F.; Methodology, F.G.; Project administration, A.F.; Resources, S.M.; Software, F.F.; Supervision, A.F. and S.M.; Validation, F.F.; Visualization, P.P.; Writing—original draft, F.G. and P.P.; Writing—review & editing, A.P.; Writing – review & editing, M.F.

Funding: This research was funded by research grant Pietro della Valle by Italian Ministry of Instruction University and research (MIUR).

Conflicts of Interest: The authors declare no conflict of interest.

References

1. Owe, M.; de Jeu, R.; Walker, J. A methodology for surface soil moisture and vegetation optical depth retrieval using the microwave polarization difference index. *IEEE Trans. Geosci. Remote Sens.* **2001**, *39*, 1643–1654. [CrossRef]
2. Seneviratne, S.I.; Corti, T.; Davin, E.L.; Hirschi, M.; Jaeger, E.B.; Lehner, I.; Orlowsky, B.; Teuling, A.J. Investigating soil moisture–climate interactions in a changing climate: A review. *Earth Sci. Rev.* **2010**, *99*, 125–161. [CrossRef]
3. Koster, R.D.; Dirmeyer, P.A.; Guo, Z.; Bonan, G.; Chan, E.; Cox, P.; Gordon, C.; Kanae, S.; Kowalczyk, E.; Lawrence, D. Regions of strong coupling between soil moisture and precipitation. *Science* **2004**, *305*, 1138–1140. [CrossRef] [PubMed]
4. Petropoulos, G.P.; Ireland, G.; Barrett, B. Surface soil moisture retrievals from remote sensing: Current status, products & future trends. *Phys. Chem. Earth* **2015**, *83*, 36–56.
5. Manfreda, S.; McCabe, M.F.; Fiorentino, M.; Rodríguez-Iturbe, I.; Wood, E.F. Scaling characteristics of spatial patterns of soil moisture from distributed modelling. *Adv. Water Resour.* **2007**, *30*, 2145–2150. [CrossRef]
6. Engman, E.T. Applications of microwave remote sensing of soil moisture for water resources and agriculture. *Remote Sens. Environ.* **1991**, *35*, 213–226. [CrossRef]
7. Entekhabi, D.; Nakamura, H.; Njoku, E.G. Solving the inverse problem for soil moisture and temperature profiles by sequential assimilation of multifrequency remotely sensed observations. *IEEE Trans. Geosci. Remote Sens.* **1994**, *32*, 438–448. [CrossRef]

8. Bolten, J.D.; Crow, W.T.; Zhan, X.; Jackson, T.J.; Reynolds, C.A. Evaluating the utility of remotely sensed soil moisture retrievals for operational agricultural drought monitoring. *IEEE J. Sel. Top. Appl. Earth Obs. Remote Sens.* **2010**, *3*, 57–66. [CrossRef]
9. Albergel, C.; Rüdiger, C.; Pellarin, T.; Calvet, J.-C.; Fritz, N.; Froissard, F.; Suquia, D.; Petitpa, A.; Piguet, B.; Martin, E. From near-surface to root-zone soil moisture using an exponential filter: An assessment of the method based on in situ observations and model simulations. *Hydrol. Earth Syst. Sci.* **2008**, *12*, 1323–1337. [CrossRef]
10. Ford, T.; Harris, E.; Quiring, S. Estimating root zone soil moisture using near-surface observations from SMOS. *Hydrol. Earth Syst. Sci.* **2014**, *18*, 139–154. [CrossRef]
11. Zhao, W.; Li, A. A comparison study on empirical microwave soil moisture downscaling methods based on the integration of microwave-optical/IR data on the Tibetan Plateau. *Int. J. Remote Sens.* **2015**, *36*, 4986–5002. [CrossRef]
12. Wang, L.; Qu, J.J. Satellite remote sensing applications for surface soil moisture monitoring: A review. *Front. Earth Sci.* **2009**, *3*, 237–247. [CrossRef]
13. Jackson, T.J., III. Measuring surface soil moisture using passive microwave remote sensing. *Hydrol. Process* **1993**, *7*, 139–152. [CrossRef]
14. Kim, H.; Lakshmi, V. Use of Cyclone Global Navigation Satellite System (CYGNSS) observations for estimation of soil moisture. *Geophys. Res. Lett.* **2018**, *45*, 8272–8282. [CrossRef]
15. Wagner, W.; Hahn, S.; Kidd, R.; Melzer, T.; Bartalis, Z.; Hasenauer, S.; Figa-Saldaña, J.; de Rosnay, P.; Jann, A.; Schneider, S. The ASCAT soil moisture product: A review of its specifications, validation results, and emerging applications. *Meteorol. Z.* **2013**, *22*, 5–33. [CrossRef]
16. Burgin, M.S.; Colliander, A.; Njoku, E.G.; Chan, S.K.; Cabot, F.; Kerr, Y.H.; Bindlish, R.; Jackson, T.J.; Entekhabi, D.; Yueh, S.H. A comparative study of the SMAP passive soil moisture product with existing satellite-based soil moisture products. *IEEE Trans. Geosci. Remote Sens.* **2017**, *55*, 2959–2971. [CrossRef]
17. Massari, C.; Camici, S.; Ciabatta, L.; Brocca, L. Exploiting satellite-based surface soil moisture for flood forecasting in the Mediterranean area: State update versus rainfall correction. *Remote Sens.* **2018**, *10*, 292. [CrossRef]
18. Alvarez-Garreton, C.; Ryu, D.; Western, A.W.; Crow, W.T.; Su, C.H.; Robertson, D.R. Dual assimilation of satellite soil moisture to improve streamflow prediction in data-scarce catchments. *Water Resour. Res.* **2016**, *52*, 5357–5375. [CrossRef]
19. Laiolo, P.; Gabellani, S.; Campo, L.; Silvestro, F.; Delogu, F.; Rudari, R.; Pulvirenti, L.; Boni, G.; Fascetti, F.; Pierdicca, N. Impact of different satellite soil moisture products on the predictions of a continuous distributed hydrological model. *Int. J. Appl. Earth Obs. Geoinf.* **2016**, *48*, 131–145. [CrossRef]
20. Brocca, L.; Ciabatta, L.; Massari, C.; Camici, S.; Tarpanelli, A. Soil moisture for hydrological applications: Open questions and new opportunities. *Water* **2017**, *9*, 140. [CrossRef]
21. Wright, A.J.; Walker, J.P.; Pauwels, V.R. Identification of Hydrologic Models, Optimized Parameters, and Rainfall Inputs Consistent with In Situ Streamflow and Rainfall and Remotely Sensed Soil Moisture. *J. Hydrometeorol.* **2018**, *19*, 1305–1320. [CrossRef]
22. Koster, R.D.; Brocca, L.; Crow, W.T.; Burgin, M.S.; De Lannoy, G.J. Precipitation estimation using L-band and C-band soil moisture retrievals. *Water Resour. Res.* **2016**, *52*, 7213–7225. [CrossRef] [PubMed]
23. Ford, T.W.; Quiring, S.M.; Thakur, B.; Jogineedi, R.; Houston, A.; Yuan, S.; Kalra, A.; Lock, N. Evaluating Soil Moisture–Precipitation Interactions Using Remote Sensing: A Sensitivity Analysis. *J. Hydrometeorol.* **2018**, *19*, 1237–1253. [CrossRef]
24. Martínez-Fernández, J.; González-Zamora, A.; Sánchez, N.; Gumuzzio, A.; Herrero-Jiménez, C. Satellite soil moisture for agricultural drought monitoring: Assessment of the SMOS derived Soil Water Deficit Index. *Remote Sens. Environ.* **2016**, *177*, 277–286. [CrossRef]
25. Mishra, A.; Vu, T.; Veettil, A.V.; Entekhabi, D. Drought monitoring with soil moisture active passive (SMAP) measurements. *J. Hydrol.* **2017**, *552*, 620–632. [CrossRef]
26. Koster, R.; Crow, W.; Reichle, R.; Mahanama, S.P. Estimating Basin-Scale Water Budgets with SMAP Level 2 Soil Moisture Data. *Water Resour. Res.* **2018**, *54*, 4228–4244. [CrossRef] [PubMed]
27. Jackson, T.J.; Schmugge, T.J. Passive microwave remote sensing system for soil moisture: Some supporting research. *IEEE Trans. Geosci. Remote Sens.* **1989**, *27*, 225–235. [CrossRef]

28. Zohaib, M.; Kim, H.; Choi, M. Evaluating the patterns of spatiotemporal trends of root zone soil moisture in major climate regions in East Asia. *J. Geophys. Res. Atmos.* **2017**, *122*, 7705–7722. [CrossRef]
29. Akbar, R.; Chen, R.; Tabatabaeenejad, A.; Moghaddam, M. Synergistic use of AirMOSS P-band SAR with the SMAP L-band radar-radiometer for soil moisture retrieval. In Proceedings of the 2016 International Conference on Electromagnetics in Advanced Applications (ICEAA), Cairns, QLD, Australia, 19–23 September 2016; pp. 793–795.
30. Chapin, E.; Chau, A.; Chen, J.; Heavey, B.; Hensley, S.; Lou, Y.; Machuzak, R.; Moghaddam, M. AirMOSS: An Airborne P-band SAR to measure root-zone soil moisture. In Proceedings of the IEEE Radar Conference, Atlanta, GA, USA, 7–11 May 2012; pp. 0693–0698.
31. Wagner, W.; Lemoine, G.; Rott, H. A method for estimating soil moisture from ERS scatterometer and soil data. *Remote Sens. Environ.* **1999**, *70*, 191–207. [CrossRef]
32. Faridani, F.; Farid, A.; Ansari, H.; Manfreda, S. Estimation of the root-zone soil moisture using passive microwave remote sensing and SMAR Model. *J. Irrig. Drain. Eng.* **2016**, *143*, 04016070. [CrossRef]
33. Manfreda, S.; Brocca, L.; Moramarco, T.; Melone, F.; Sheffield, J. A physically based approach for the estimation of root-zone soil moisture from surface measurements. *Hydrol. Earth Syst. Sci.* **2014**, *18*, 1199–1212. [CrossRef]
34. Faridani, F.; Farid, A.; Ansari, H.; Manfreda, S. A modified version of the SMAR model for estimating root-zone soil moisture from time-series of surface soil moisture. *Water SA* **2017**, *43*, 492–498. [CrossRef]
35. Baldwin, D.; Manfreda, S.; Keller, K.; Smithwick, E. Predicting root zone soil moisture with soil properties and satellite near-surface moisture data across the conterminous United States. *J. Hydrol.* **2017**, *546*, 393–404. [CrossRef]
36. Fereidoon, M.; Koch, M.; Brocca, L. Predicting rainfall and runoff through satellite soil moisture data and SWAT modelling for a poorly gauged basin in Iran. *J. Hydrol.* **2018**, *11*, 594. [CrossRef]
37. Araghi, A.; Baygi, M.M.; Adamowski, J.; Malard, J.; Nalley, D.; Hasheminia, S.M. Using wavelet transforms to estimate surface temperature trends and dominant periodicities in Iran based on gridded reanalysis data. *Atmos. Res.* **2015**, *155*, 52–72. [CrossRef]
38. Golian, S.; Mazdiyasni, O.; AghaKouchak, A. Trends in meteorological and agricultural droughts in Iran. *Appl. Clim.* **2015**, *119*, 679–688. [CrossRef]
39. Tabari, H.; Abghari, H.; Hosseinzadeh Talaee, P. Temporal trends and spatial characteristics of drought and rainfall in arid and semiarid regions of Iran. *Hydrol. Process* **2012**, *26*, 3351–3361. [CrossRef]
40. Tabari, H.; Nikbakht, J.; Talaee, P.H. Hydrological drought assessment in Northwestern Iran based on streamflow drought index (SDI). *Water Resour. Manag.* **2013**, *27*, 137–151. [CrossRef]
41. Rahmani, A.; Golian, S.; Brocca, L. Multiyear monitoring of soil moisture over Iran through satellite and reanalysis soil moisture products. *Int. J. Appl. Earth Obs. Geoinf.* **2016**, *48*, 85–95. [CrossRef]
42. Modarres, R.; Sarhadi, A. Rainfall trends analysis of Iran in the last half of the twentieth century. *J. Geophys. Res. Atmos* **2009**, *114*, D03101. [CrossRef]
43. Safaei-Mahroo, B.; Ghaffari, H.; Fahimi, H.; Broomand, S.; Yazdanian, M.; Najafi-Majd, E.; Hosseinian Yousefkhani, S.S.; Rezazadeh, E.; Hosseinzadeh, M.S.; Nasrabadi, R. The herpetofauna of Iran: Checklist of taxonomy, distribution and conservation status. *AHR* **2015**, *6*, 257–290.
44. INSAM—The International Society for Agricultural Meteorology. Available online: http://www.agrometeorology.org/ (accessed on 29 January 2019).
45. WMO—World Meteorological Organization. Available online: https://www.wmo.int/cpdb/iran-islamic-republic-of (accessed on 10 March 2018).
46. Njoku, E.G.; Jackson, T.J.; Lakshmi, V.; Chan, T.K.; Nghiem, S.V. Soil moisture retrieval from AMSR-E. *IEEE Trans. Geosci. Remote Sens.* **2003**, *41*, 215–229. [CrossRef]
47. Kerr, Y.H.; Waldteufel, P.; Wigneron, J.-P.; Martinuzzi, J.; Font, J.; Berger, M. Soil moisture retrieval from space: The Soil Moisture and Ocean Salinity (SMOS) mission. *IEEE Trans. Geosci. Remote Sens.* **2001**, *39*, 1729–1735. [CrossRef]
48. Entekhabi, D.; Njoku, E.G.; O'Neill, P.E.; Kellogg, K.H.; Crow, W.T.; Edelstein, W.N.; Entin, J.K.; Goodman, S.D.; Jackson, T.J.; Johnson, J. The soil moisture active passive (SMAP) mission. *Proc. IEEE* **2010**, *98*, 704–716. [CrossRef]
49. Imaoka, K.; Kachi, M.; Kasahara, M.; Ito, N.; Nakagawa, K.; Oki, T. Instrument performance and calibration of AMSR-E and AMSR2. *Int. Arch. Photogramm. Remote Sens. Spat. Inf. Sci.* **2010**, *38*, 13–18.

50. Kim, H.; Parinussa, R.; Konings, A.G.; Wagner, W.; Cosh, M.H.; Lakshmi, V.; Zohaib, M.; Choi, M. Global-scale assessment and combination of SMAP with ASCAT (active) and AMSR2 (passive) soil moisture products. *Remote Sens. Environ.* **2018**, *204*, 260–275. [CrossRef]
51. Goddard Earth Sciences Data and Information Services Center (GES Disc). Available online: https://disc.gsfc.nasa.gov (accessed on 20 April 2018).
52. Monerris, A.; Schmugge, T. Soil moisture estimation using L-band radiometry. In *Advances in Geoscience and Remote Sensing*; IntechOpen: London, UK, 2009.
53. Mecklenburg, S.; Drusch, M.; Kaleschke, L.; Rodriguez-Fernandez, N.; Reul, N.; Kerr, Y.; Font, J.; Martin-Neira, M.; Oliva, R.; Daganzo-Eusebio, E. ESA's Soil Moisture and Ocean Salinity mission: From science to operational applications. *Remote Sens. Environ.* **2016**, *180*, 3–18. [CrossRef]
54. Centre Aval de Traitement des Données SMOS (CATDS). Available online: https://www.catds.fr/ (accessed on 30 April 2018).
55. National Snow and Ice Data Center (NSIDC). Available online: http://nsidc.org/data/SPL3SMP (accessed on 10 May 2018).
56. Entekhabi, D.; Reichle, R.H.; Koster, R.D.; Crow, W.T. Performance metrics for soil moisture retrievals and application requirements. *J. Hydrometeorol.* **2010**, *11*, 832–840. [CrossRef]
57. Kim, S.; Liu, Y.Y.; Johnson, F.M.; Parinussa, R.M.; Sharma, A. A global comparison of alternate AMSR2 soil moisture products: Why do they differ? *Remote Sens. Environ.* **2015**, *161*, 43–62. [CrossRef]
58. Ray, R.; Fares, A.; He, Y.; Temimi, M. Evaluation and inter-comparison of satellite soil moisture products using in situ observations over Texas, US. *Water* **2017**, *9*, 372. [CrossRef]
59. Oliva, R.; Daganzo, E.; Kerr, Y.H.; Mecklenburg, S.; Nieto, S.; Richaume, P.; Gruhier, C. SMOS radio frequency interference scenario: Status and actions taken to improve the RFI environment in the 1400–1427-MHz passive band. *IEEE Trans. Geosci. Remote Sens.* **2012**, *50*, 1427–1439. [CrossRef]
60. Khazâal, A.; Cabot, F.; Anterrieu, E.; Soldo, Y. A kurtosis-based approach to detect RFI in SMOS image reconstruction data processor. *IEEE Trans. Geosci. Remote Sens.* **2014**, *52*, 7038–7047. [CrossRef]
61. Cui, H.; Jiang, L.; Du, J.; Zhao, S.; Wang, G.; Lu, Z.; Wang, J. Evaluation and analysis of AMSR-2, SMOS, and SMAP soil moisture products in the Genhe area of China. *J. Geophys. Res. Atmos* **2017**, *122*, 8650–8666. [CrossRef]
62. Chen, Y.; Yang, K.; Qin, J.; Cui, Q.; Lu, H.; La, Z.; Han, M.; Tang, W. Evaluation of SMAP, SMOS, and AMSR2 soil moisture retrievals against observations from two networks on the Tibetan Plateau. *J. Geophys. Res. Atmos.* **2017**, *122*, 5780–5792. [CrossRef]
63. Zhang, X.; Zhang, T.; Zhou, P.; Shao, Y.; Gao, S. Validation analysis of SMAP and AMSR2 soil moisture products over the United States using ground-based measurements. *Remote Sens.* **2017**, *9*, 104. [CrossRef]